Journal of Applied Geophysics 80 (2012) 83–90

Contents lists available at SciVerse ScienceDirect

Journal of Applied Geophysics

journal homepage: www.elsevier.com/locate/jappgeo

Measured electric responses of unconsolidated layered and brine-saturated sand and sand-clay packs under continuous fluid flow conditions

M. Kavian [a,*], E.C. Slob [a], W.A. Mulder [a,b]

[a] Department of Geotechnology, Delft University of Technology, Stevinweg 1, 2628 CN Delft, The Netherlands
[b] Shell Global Solutions International BV, PO Box 60, 2280 AB Rijswijk, The Netherlands

ARTICLE INFO

Article history:
Received 18 April 2011
Accepted 30 January 2012
Available online 8 February 2012

Keywords:
Complex electric measurements
Unconsolidated layered sand-clay
Salinity
Electric hysteresis
Double Cole–Cole model

ABSTRACT

We have investigated the effects of pore solution concentration on the complex electric response of two different unconsolidated samples, layered sand and sand-clay in the frequency range from 30 kHz to 3 MHz. The electric parameters that describe the electric response of the samples—real part of permittivity, conductivity amplitude and phase—are obtained through two-electrode electric measurements. Plots of the conductivity amplitude and phase as a function of frequency show large variations with water saturation and NaCl concentrations. This sensitivity may be useful for the characterization of the vadose zone. Under continuous fluid flow conditions, first drainage and secondary imbibition cycles were conducted for the two three-layered samples saturated with saline water in three different NaCl solution concentrations at atmospheric pressure and temperatures between 21 °C and 22 °C. Electrode polarization distorted the measurements, particularly in the kHz range. The distortion becomes negligible above a limiting lower frequency, which depends on NaCl solution concentration and the kind of sample. To obtain the intrinsic behaviour of the samples, the electric permittivities were analyzed above the limiting frequencies. Analysis of the real part of electric permittivity versus saturation indicates that, with increasing salinity concentration, the real part of the electric permittivity increases. Also, the hysteretic effect, the difference between first drainage and second imbibition, becomes more pronounced and remains present at higher frequencies. For the two samples, we observed a different correlation between conductivity amplitude/phase spectra and pore fluid concentration for seven saturation levels, suggesting that conductivity amplitude/phase spectra contain information about water saturation, salt solution concentration, and geotechnical properties (e.g., fines content) of unconsolidated near-surface soils. A simplified five-parameter double Cole–Cole model could fit the experimental data.

1. Introduction

Electric laboratory measurements of soil samples, carried out to assess the effect of water saturation, mineralogy, grain size distribution, and electrolyte concentration, are relevant for many hydrological and environmental studies.

Low-frequency electromagnetic (EM) fields that diffuse through the subsurface are influenced by time-relaxation phenomena, resulting in a frequency-dependent effect. Especially in clays, peat, and minerals, electric frequency-dependent effects can be strong. Many electric measurements have been done to study the electric phenomena in porous media such as unconsolidated sand (Shahidi et al., 1975; Ulrich and Slater, 2004) and sandstones (Binley et al., 2005; Knight, 1991). Laboratory measurements of complex impedance in the frequency range of 10 mHz to 10 MHz are available for saturated soils made from mixtures of sand and clay. The governing polarization mechanisms are different over this broad range of frequencies. The membrane polarization model introduced by Marshall and Madden (1959) plays an important role at frequencies below 1 Hz. Membrane polarization is due to differences in mobility between anions and cations in adjacent clay-bound and clay-free zones in pore paths (Klein and Sill, 1982; Ward and Fraser, 1967). At higher frequencies (e.g., above 10 Hz), the polarization effects have been related to different mechanisms. These mechanisms are: clay counterion displacement (Vinegar and Waxman, 1984), the Maxwell–Wagner effect (also called interfacial polarization) or ionic double-layer (Garrouch and Sharma, 1994; Lima and Sharma, 1992; Olhoeft, 1985; Schön, 1996; Vanhala and Soininen, 1995; Ward, 1990). The near surface, more specifically the first few hundred meters, is a region where strong frequency-dependent effects can occur and where large-scale interactions between different layers can lead to large-scale electric effects. On a laboratory scale, the frequency dependence of the electric properties for layered unconsolidated sand-clays has rarely been studied for different NaCl solution concentrations. Recently, the investigation of unconsolidated sands and clays became of interest for environmental, engineering and hydrogeological applications, such as infiltration and subsequent displacement of water-

* Corresponding author. Tel.: +31 15 278 39 87; fax: +31 15 278 11 89.
E-mail addresses: m.kavian@tudelft.nl, mohsenkav@yahoo.com (M. Kavian).

0926-9851/$ – see front matter © 2012 Elsevier B.V. All rights reserved.
doi:10.1016/j.jappgeo.2012.01.012

immiscible contaminants in natural ground water flow, underground sites for waste disposal, and buildings projects. In this paper, we focus on the electric behaviour of brine-saturated layered unconsolidated sand and sand-clay in the frequency range of 30 kHz to 3 MHz. One application could be borehole logging data, because the frequency range and physical scale that we use are similar to those used in borehole logging.

The frequency dependence of the measurements is not the only characteristic of interest, but also the electric hysteretic effect, which can be defined as the difference in electric permittivity values between the first drainage and the secondary imbibition cycles. Hysteresis implies that information about water content from geophysical data sets can depend on the saturation history (Knight and Nur, 1987).

As a consequence, the electric response of a medium contains information about the pore fluid distributions in a heterogeneous porous medium. Chelidze et al. (1999) related this hysteretic behaviour to the pore-scale fluid distribution during drainage and imbibition. Laboratory experiments on sandstone reported by Knight (1991) show that measured values of electric resistivity can depend on the saturation history of the sandstone samples in a specified range of saturations. Knight and Nur (1987) found electric permittivity hysteresis between drainage and imbibition while they used a static technique rather than a dynamic technique to do the saturation cycles. In the static technique, the electric measurements are conducted in the absence of pore fluid flow, whereas in the dynamic technique, the measurements are performed under flowing conditions. We found that, during saturation of the samples, the dynamic technique could produce different electric results than the static technique (Kavian et al., 2011).

The electric permittivity hysteresis must be caused by a change in the gradient of the water saturation. This led Plug et al. (2007a) to formulate the hypothesis that the difference in water saturation gradient should be observable in the capillary pressure.

The questions we considered are whether the change in pore salinity concentration influences the electric hysteretic effects at different frequencies and whether these effects in the presence of the clay fraction are of the same nature as those in sand packs. To find the answers to these questions, we measured the complex electric permittivities of sand and sand-clay samples in wet cases to establish the factors affecting their electric response. We investigated unconsolidated three-layered sand as well as a three-layered sand-clay sample during first drainage and secondary imbibition of water at three different NaCl solution concentrations. We conducted the experiment for layered models, using sands of different grain sizes and an artificial clay powder.

The experiments are similar to those reported for homogeneous unconsolidated coarse sand (Plug et al., 2007a) or sandstone (Knight and Nur, 1987) using distilled water as saturating fluid or homogeneous or layered sand (Kavian et al., 2011) saturated with water of various salinities.

Here, we extend these experiments by introducing layered unconsolidated sand-clay packs and by considering different NaCl concentrations under pore fluid flow conditions.

We will first describe the measurement procedures, the processing of the measured data, and the choice of samples. The samples were sequentially saturated with water of three different NaCl solution concentrations (1 mmol/l, 10 mmol/l, and 100 mmol/l).

Then, we will present the results as a function of frequency, in the form of complex electric permittivities as well as amplitudes and phases of the electric conductivity, for three-layered sand and sand-clay samples. Here we show the best fit of a simplified five-parameter double Cole–Cole model that we applied to two different unconsolidated three-layered samples for all water saturation levels and the three salt concentrations used.

2. Experimental procedure

We used two different coarse- and fine-grained unconsolidated quartz sands, named S350 and S150, respectively, with an average grain size ranging from 350 μm to 420 μm and 150 μm to 175 μm. For the clay, we selected an artificial clay powder, WWB111, named Clay, which consists for 63% of quartz and 27% of alumina and with an average grain size of 2 μm to 10 μm and specific surface area of 10 m^2/g. A drawing of the sample holder is shown in Fig. 1(left) and can be used with a maximum of five 30 mm high PVC rings, each with a diameter of 150 mm. It has two non-conductive PVC end pieces, containing the water inlet and outlet, and two metal porous plates, which are placed inside the end pieces and act as electrodes (Kavian et al., 2011). When the sample holder is filled with the dry samples, it is vibrated for 15 minutes to reach a porosity of 0.375 ± 0.005, 0.395 ± 0.005, and 0.65 ± 0.005 for the coarse- and fine-grain sands, and clay, respectively (Plug and Bruining, 2007). For further reference we use three letter short-hand notation for the layered packs as described in Table 1. The two three-layered cases are defined, respectively, as CFC and BFC, where C, F, and B stand for the coarse, fine, and clay as defined in Table 1. In the right-pane of Fig. 1, a picture of the BFC is shown.

To measure the relative effective complex permittivity, a component analyzer (Wayne–Kerr, 6640A) is connected to the two end electrodes. It measures the impedance amplitude, $|Z|$ [Ω], and the phase angle, φ [rad], as a function of frequency. The complex impedance measurements, $Z = Z_r - \iota Z_i$, are related to the relative effective complex permittivity, ε, of the sample, defined by $\varepsilon = \varepsilon_r - \iota\varepsilon_i$, where ι denotes the imaginary unit and the indices $_r$ and $_i$ represent the real and imaginary parts, respectively. The measurements can also be expressed in terms of a conductivity magnitude, $|\sigma|$, and a phase angle, φ:

$$|\sigma^*| = \sqrt{\sigma_r^2 + \sigma_i^2}, \tag{1}$$

$$\varphi = \arctan\left(\frac{\sigma_i}{\sigma_r}\right), \tag{2}$$

where the real part of conductivity σ_r represents the ability to conduct an electric current and the imaginary part σ_i represents the ability to polarize charges (capacitance effect). The imaginary part of the complex permittivity can be further split into two parts, one containing polarization effects and another describing a dc-conductivity, $\varepsilon_i = \varepsilon_{pl}(\omega) + \sigma_{dc}/(\varepsilon_0\omega)$, where, ε_0 is the permittivity in a vacuum and ω is the angular frequency, defined by $\omega = 2\pi f$ for natural frequency f. We used air measurements to correct for the capacitance of residual contributions, caused by the setup. A complete description of the setup, calibration, data validation, and experimental procedure can be found in Kavian et al. (2011).

To conduct drainage-imbibition cycles, we first saturated the sample with a NaCl solution with a concentration of C = 1 mmol/l under continuous fluid flow conditions. Then in the next stage, the first drainage cycle started with a constant flow rate of 2 ml/min using a syringe pump. This first drainage cycle was continued until the flow stopped after air breakthrough, when the pump could not further remove water from the sample.

After a preparation time of 10 to 20 min to reverse the flow direction, the second imbibition cycle was initiated with the same constant flow rate as used for drainage using new saline water. The electric measurements ran almost continuously during the saturation and first desaturation cycles, for three different concentrations of salt, 1 mmol/l, 10 mmol/l, and 100 mmol/l.

In the following sections, we discuss the observed changes in the complex electric measurements associated with varying saline–water saturations and various degrees of heterogeneity.

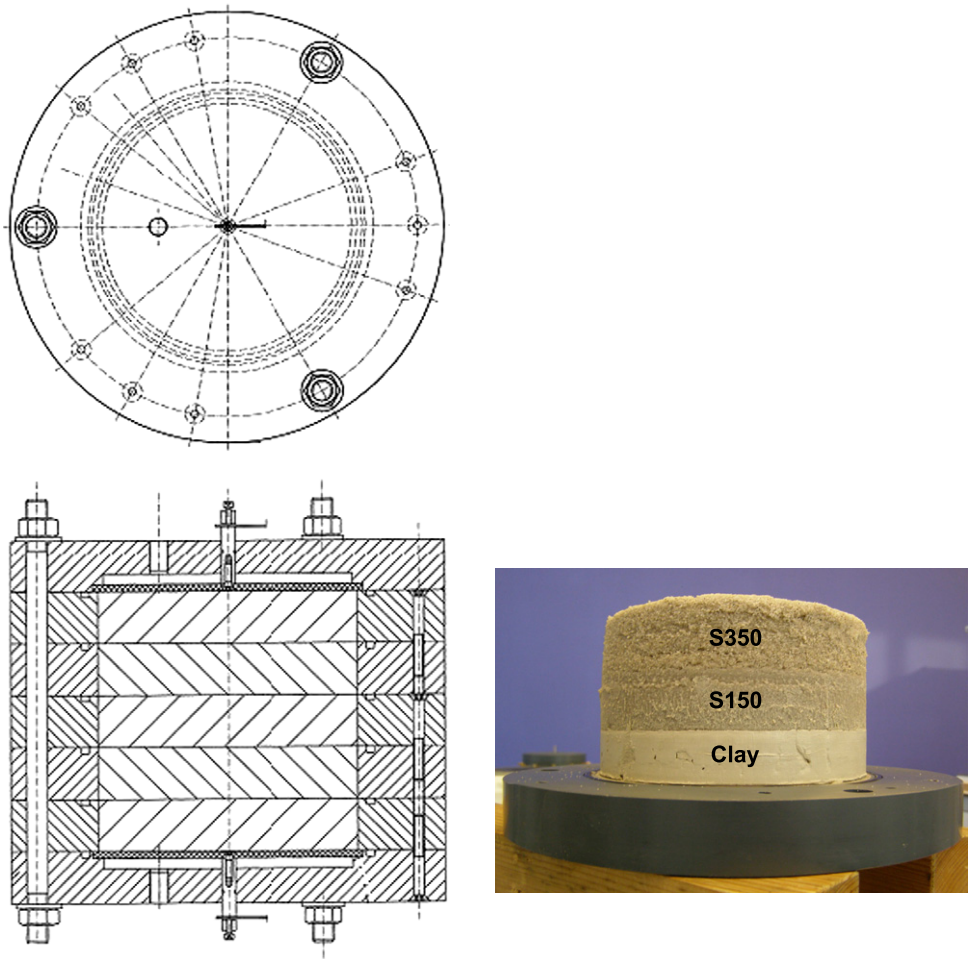

Fig. 1. (Left) Cross section of the sample holder: top and front view; (right) picture of a three-layered sand-clay. This picture was taken after last drainage by carefully removing the PVC rings.

3. Experimental results and discussion

3.1. Effect of salinity and frequency on drainage-imbibition hysteresis of electric permittivity

Fig. 2 shows three plots of the real part of the electric permittivity versus water saturation for the three-layered sand CFC partially saturated with water containing 1 mmol/l (a), 10 mmol/l (b), and 100 mmol/l (c) salt concentrations. In each plot, results are shown at frequencies 105 kHz, 332 kHz, 105 MHz, and 3 MHz for first drainage and second imbibition cycles. At the highest concentration of $C = 100$ mmol/l, we consider 1.67 MHz instead of 3 MHz because of the low accuracy of our measuring equipment for this high salt concentration. By comparing the results in Fig. 2a), b), and c), three observations can be made. With increasing salinity the real part of the electric permittivity increases, the difference between drainage and imbibition curves increases, and the hysteresis becomes more pronounced at higher frequencies. Fig. 3 shows similar results obtained with the BFC sample. By comparing the results for the three different salt concentrations, we see that the presence of the fine sand and clay fractions reduces the hysteretic effect significantly, but the three observations made with the previous layered sample remain valid. The sharp drop in the permittivity values at high saturation levels can be explained with percolation theory as discussed by Chelidze and Gueguen (1999). According to this theory, when a continuous conducting path of water is formed, the capacitive contribution from the water-air capacitors is effectively short-circuited whereas the water–grain capacitors still have a contribution to the real part of the permittivity of the sample.

Table 1
Three letter acronyms for the three-layered packs, with constituents named from left to right in the acronyms from bottom to top as in the layered samples.

	Sample	
Layer	CFC	BFC
Top	S350	S350
Middle	S150	S150
Bottom	S350	Clay

The major difference between the layered sand sample and the layered sand-clay sample is that the imbibition curves are always above the drainage curves for CFC sample, whereas it is the opposite for the BFC sample. Knight and Nur (1987) and Plug et al. (2007b) reported on experiments in the kilohertz to megahertz frequency range on sandstone and homogeneous coarse-grain unconsolidated sand, respectively. They saturated their samples with deionized water and found that the ε_r during second imbibition has higher values than during first drainage.

They ascribed the low-frequency ε_r behaviour to the polarization of both the gas–water and water–grain interfaces (interfacial polarization mechanisms), which occurs during drainage and imbibition cycles with different bulk phase geometries and distributions. Knight and Nur (1987) attributed the electric hysteresis to capacitive charging and discharging of gas pockets that is more enhanced during imbibition than during drainage. Ulrich and Slater (2004) did measurements on

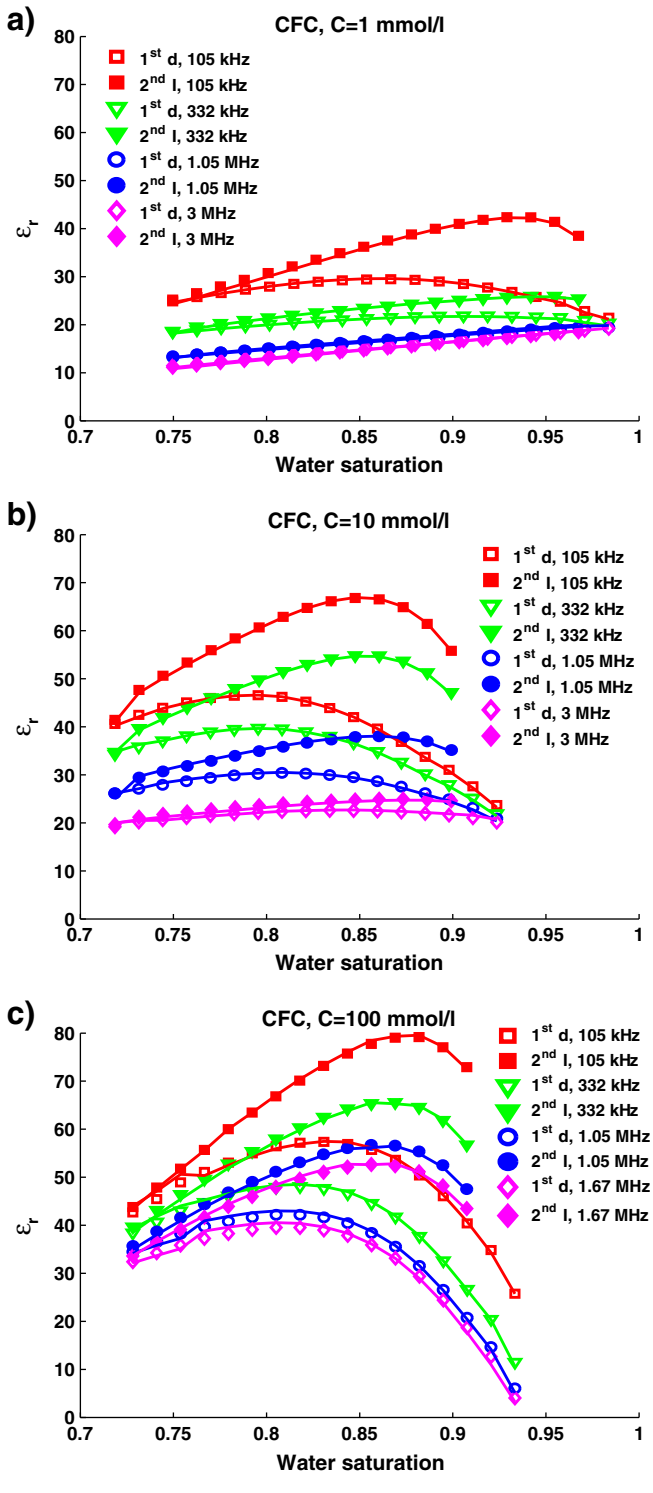

Fig. 2. Hysteresis in the real part of the complex electric permittivity for a three-layered unconsolidated sand pack with average grain size of 150 μm in the middle and 350 μm at the top and bottom at four different frequencies and three NaCl concentrations, (a) $C=1$ mmol/l, (b) $C=10$ mmol/l, and (c) $C=100$ mmol/l. "d" and "I" stand for drainage and imbibition processes, respectively. The modeled results are shown by solid lines.

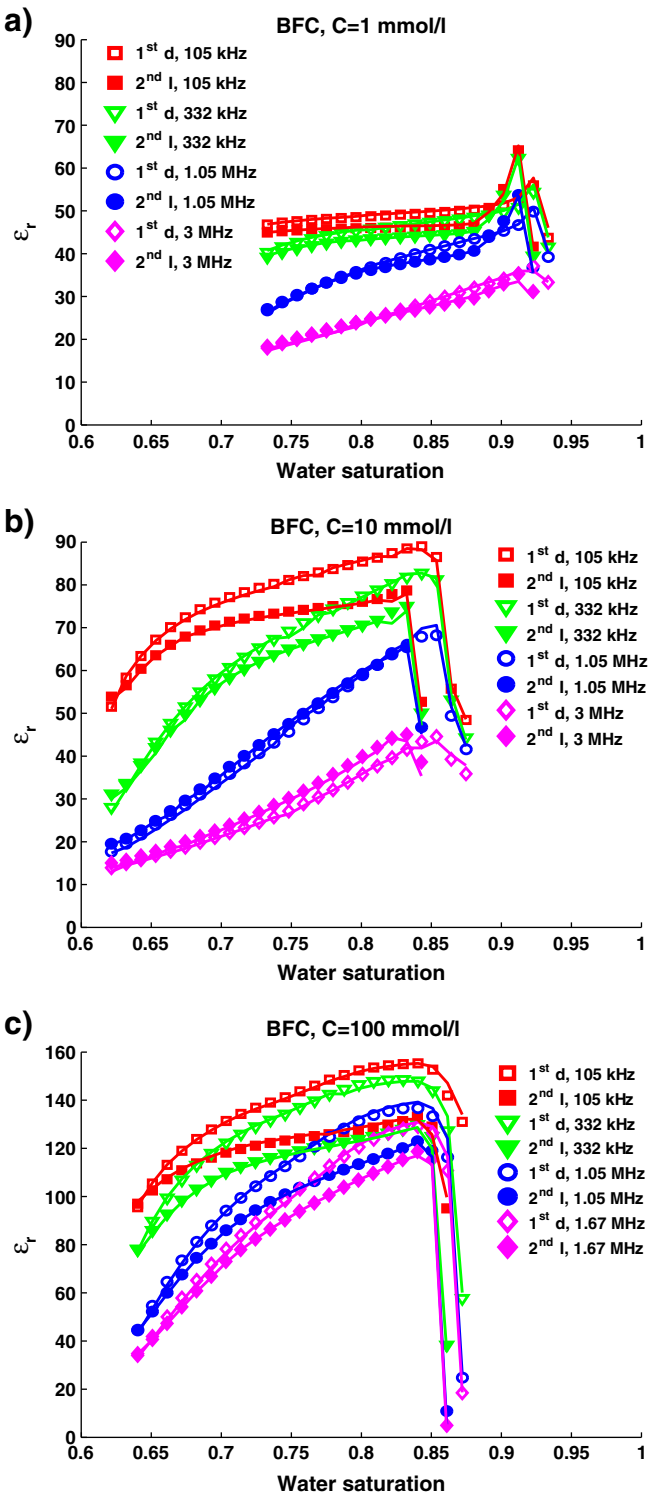

Fig. 3. Hysteresis in the real part of complex electric permittivity for a three-layered unconsolidated sand-clay pack with average grain size of 150 μm in the middle, 350 μm at the top, and clay (WWB111) at the bottom for four different frequencies and (a) $C=1$ mmol/l, (b) $C=10$ mmol/l, and (c) $C=100$ mmol/l NaCl solution concentrations. "d" and "I" stand for drainage and imbibition processes, respectively. The modeled results are shown by solid lines.

unconsolidated sand in the low-frequency range (0.1–1000 Hz) and used Knight's idea to interpret the larger values of polarization found during imbibition with respect to the drainage cycle. Our results indicate that the distribution of pore fluids during saturation and desaturation cycles depend on the presence of clay particles in layered samples.

3.2. Dependence of electric conductivity on salinity and water saturation as a function of frequency

We considered the effect of salinity and water saturation on the electric conductivity spectra. The amplitude and phase of the conductivity

are shown in Figs. 4 and 5 for seven different water saturation levels and for three NaCl concentrations, for a three-layered unconsolidated sand as well as for the sand-clay samples.

The electric conductivity amplitudes, shown in Fig. 4(a), hardly depend on frequency at low frequencies but vary with salinity concentration and water saturation.

At higher frequencies, the electric conductivity amplitudes start to increase. The transition from constant to increasing occurs at a frequency that is higher for larger conductivities.

Fig. 4b) shows the behaviour of the phase spectra for frequencies above 30 kHz. The phase plots display a simple polynomial increase with the logarithm of the frequency.

The 10 mmol/l line at 83% saturation of the BFC curve in Fig. 5a) corresponds in conductivity value and behaviour to the 1 mmol/l at 74% saturation of the CFC curve in Fig. 4a). The major difference is that for the BFC sample the conductivity amplitude increases faster than for the CFC sample at the same low-frequency conductivity value. This implies that the steepness of the conductivity's amplitude increase with increasing frequency contains information about the fine fraction.

Fig. 5b) depicts the conductivity's phase spectra for the BCF sample at the three salt concentrations and the different water saturation levels. At frequencies above the range of constant conductivity amplitude, the phase starts to decrease for increasing water saturation and increasing salinity.

The phase spectra have a maximum at a certain frequency, for instance at 10 kHz for a concentration of 1 mmol/l, outside the range of the graph in Fig. 5b). We have used artificial clay (alumina) which is characterized by a very small conductivity value. This can be seen from Fig. 5b), where at 1 mmol/l concentration the phase is almost $\pi/2$. This means that the complex conductivity has a dominant imaginary part, hence the clay layer acts as a capacitor.

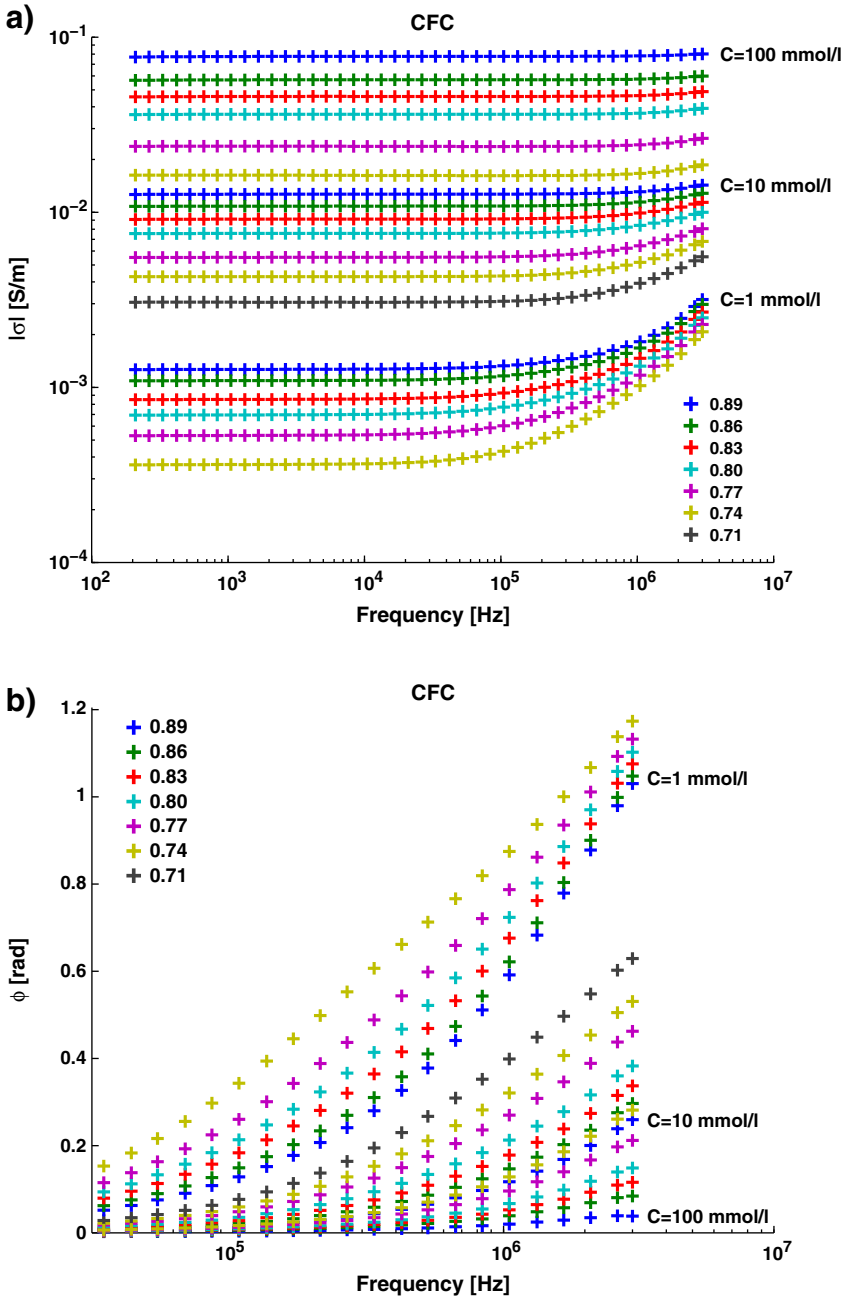

Fig. 4. (a) Amplitude and (b) phase spectra of the complex electric conductivity obtained during the drainage process for the three-layered sand sample at different saturation levels and for three different NaCl concentrations of $C=1$ mmol/l, $C=10$ mmol/l, and $C=100$ mmol/l.

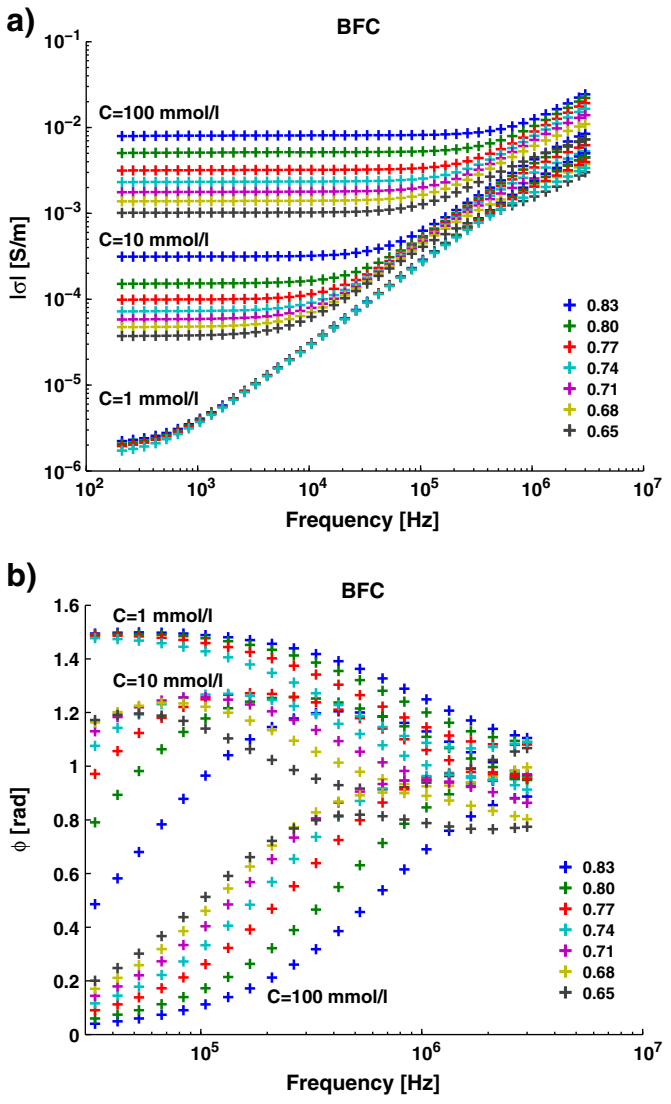

Fig. 5. (a) Amplitude and (b) phase spectra of the complex electric conductivity obtained during the drainage process for the three-layered sand-clay sample at different saturation levels and for three different NaCl concentrations of $C=1$ mmol/l, $C=10$ mmol/l, and $C=100$ mmol/l NaCl solution concentrations.

The frequency of the peak value increases with increasing salinity and water saturation. For frequencies above that of maximum phase, the phase decreases with increasing salinity concentrations. At a fixed salt concentration, however, it increases with increasing water saturation levels, a phenomenon that is opposite to that in sandstone at frequencies below 1 kHz (Binley et al., 2005). This implies that the phase, measured over a wide frequency range, carries information about salinity and water saturation, which could be of importance for vadose zone characterization.

4. Modeling of the data by means of equivalent electric circuits

For practical purposes, we can interpret our experimental data using equivalent electric circuit models. By assuming that the surface and bulk electric properties are equivalent to a parallel circuit of R_s $-(\iota\omega\chi_s)^{-\alpha}$ and a parallel classical R_b–C_b, in series, the equivalent complex impedance of the sample is $Z(\omega)=Z_s(\omega)+Z_b(\omega)$, where

$$Z_s^*(\omega)=\frac{R_s}{1+(\iota\omega\tau_s)^{\alpha}} \quad \text{and} \quad Z_b^*(\omega)=\frac{R_b}{1+\iota\omega\tau_b}, \tag{3}$$

in which $\tau_s=R_s^{\frac{1}{\alpha}}\chi_s$ and $\tau_b=R_bC_b$. Here, τ_s is the time constant of surface polarization (Lou and Zhang, 1998). The time constant τ_b characterizes the polarization that occurs in the sample bulk volume.

The parameter α is a dispersion exponent that defines the spread of the relaxation-time spectrum. The model is an extended version of the Cole–Cole model (Pelton et al., 1978). Different forms of extensions have been used by Binley et al. (2005) to correlate between spectral induced polarization and petrophysical parameters of saturated and unsaturated sandstone, by Ghorbani et al. (2009) to model the spectral induced polarization of clayey rocks during drying process, by Weller et al. (2010) to estimate normalized specific surface area from IP measurements, and by Kruschwitz et al. (2010) to investigate textural controls on the electric response of porous media. The model is consistent with the dual polarization model introduced by Kemna et al. (2000),

$$Z^*(\omega)=R_0\left[1-\sum_{k=s,b}m_k\left(1-\frac{1}{1+(\iota\omega\tau_k)^{\alpha_k}}\right)\right], \tag{4}$$

where m_k,τ_k,α_k are chargeability, relaxation time, and dispersion exponent. When we take $m_s+m_b=1$ and $\alpha_b=1$ we obtain

$$Z^*(\omega)=\frac{R_s}{1+(\iota\omega\tau_s)^{\alpha_s}}+\frac{R_b}{1+\iota\omega\tau_b}, \tag{5}$$

with new model parameters, $R_s=m_sR_0$ and $R_b=m_bR_0$. Eq. (5) is used to obtain the unknown parameters by fitting the experimental data to the model. At lower frequencies the model is not capable of fitting the data due to the electrode polarization. The model presented by Eq. (5) can be used down to 30 kHz, based on the following experiment. First we used Eq. (5) to fit data above 100 KHz, which result can predict the data down to 30 KHz. The model result obtained over the whole range above 30 kHz is the same as the model result obtained from data above 100 kHz. In our paper (Kavian et al., 2011) we showed results above 100 kHz for sand packs.

The input data used for the fitting procedure were the real and imaginary parts of the complex impedance, computed from the amplitude and phase values measured at different frequencies during drainage and imbibition processes. After fitting the experimental data to the equivalent circuit model $Z(\omega)$, we can define the five fitting parameters. The parameters obtained for CFC sample, using data for drainage and imbibition for saturations between 0.90 and 0.75 and three NaCl concentrations of 1, 10, and 100 mmol/l, are presented in Table 2. To quantify how well the model fits the complex impedance data over the frequency range, we list the global root mean square error (RMSE),

$$RMSE=\left(\frac{\sum_{\omega}|Z^*(\omega)-Z^{*obs}(\omega)|^2}{\sum_{\omega}|Z^{*obs}(\omega)|^2}\right)^{1/2}. \tag{6}$$

The model fits the real and imaginary parts of the complex impedance values to the ascribed model quite well, with an error of less than 1.1% for all three NaCl solution concentrations. In Table 2, some relaxation times at $C=100$ mmol/l are missing. Their influence on the total solution is insignificant, and hence has no meaning. This can be inferred from the overall RMSE, which is very small. At $C=100$ mmol/l concentration τ_s is negligible for drainage ($Z_s(\omega)$ is frequency independent), whereas during imbibition τ_b is negligible ($Z_b(\omega)$ is frequency independent).

Figs. 6(a) and (b) display the real and imaginary parts of the impedance data during imbibition, at the 1 mmol/l concentration, as a function of frequency and saturation and the associated relative error (Fig. 6(c) and (d)), given by

$$\frac{|\Delta Z_{r,i}^*|}{|Z_{r,i}^*|}=\frac{|Z_{r,i}^*(\omega)-Z_{r,i}^*obs(\omega)|}{|Z_{r,i}^*obs(\omega)|}, \tag{7}$$

Table 2
Model parameters for the three-layered sand sample (CFC) obtained by fitting the data for both the drainage and the imbibition cycles at three different salt concentrations: C = 1 mmol/l, C = 10 mmol/l, and C = 100 mmol/l. Letters "d" and "I" stand for first drainage and secondary imbibition cycles, respectively. Saturation levels "S_w" are common for both drainage and imbibition cycles. "RMSE" stands for root mean square error over the frequency range studied here.

S_w	C	d	I	R_s		d	I	τ_s		d	I	α_s		d	I	R_b		d	I	τ_b		d	I	RMSE	
[−]	[mmol/l]	[$\Omega\times10^2$]				[μs]				[−]				[$\Omega\times10^2$]				[μs]				[−]			
0.90	1	9.82		18.20		0.45		0.93		0.85		0.82		27.56		28.84		0.08		0.08		0.007		0.011	
	10	0.67		1.10		0.05		0.11		0.90		0.89		3.07		3.43		0.01		0.01		0.002		0.008	
	100	0.03		0.12		–		0.03		0.61		0.92		0.02		0.57		0.05		–		0.002		0.006	
0.85	1	19.15		32.40		0.52		0.77		0.84		0.81		31.13		31.18		0.09		0.09		0.009		0.011	
	10	1.15		2.13		0.09		0.15		0.90		0.88		3.95		4.17		0.01		0.01		0.006		0.008	
	100	0.03		0.35		–		0.03		0.66		0.92		0.14		0.71		0.04		–		0.004		0.006	
0.80	1	39.60		67.01		0.54		0.71		0.83		0.82		33.51		31.10		0.09		0.09		0.009		0.009	
	10	2.40		3.90		0.12		0.15		0.89		0.88		5.00		5.13		0.01		0.01		0.006		0.009	
	100	0.03		1.32		–		0.002		0.75		0.76		0.38		0.39		0.04		0.04		0.007		0.006	
0.75	1	107		134.31		0.73		0.89		0.85		0.85		33.58		34.22		0.10		0.10		0.009		0.008	
	10	5.40		8.60		0.14		0.16		0.89		0.88		6.43		6.17		0.02		0.02		0.008		0.010	
	100	1.55		2.30		0.02		0.005		0.91		0.77		1.00		1.12		–		0.05		0.006		0.008	

for the three-layered sand sample (CFC). We have chosen the imbibition cycle at the 1 mmol/l NaCl solution concentration because it showed the largest RMSE. The relative error in fits of the real and imaginary parts of the electric impedance is satisfactory at all saturation levels. We have a relative error of less than 1.1% and 3% for real and imaginary parts of impedance, respectively. We use

$$\varepsilon^*(\omega) = \frac{d}{\imath\omega\varepsilon_0 A Z^*(\omega)}, \tag{8}$$

to convert the modeled impedances to the permittivity values. Here d (m) and A (m^2) denote the sample height and cross-sectional area, respectively. The model fits of ε_r for drainage and imbibition cycles are shown in Figs. 2 and 3 by solid lines. For both layered samples, the agreement between the model and experimental data is good, taking into account the simplicity of the model. The model fits the non-monotonic behaviour observed in the ε_r for high saturation levels during drainage and imbibition cycles quite well, with the difference between the predicted and measured data of the order of 0.1%.

5. Conclusions

We have investigated by laboratory experiments how pore solution concentrations influence the complex electric permittivity/conductivity of two different unconsolidated samples, layered sand and sand-clay, in the frequency range of 30 kHz to 3 MHz. The electric parameters that describe the electric response of the samples—real part of permittivity ε_r, conductivity amplitude $|\sigma|$ and phase φ—are obtained from the electric measurements. The results indicate that the shape of the real part of the permittivity hysteresis curves in the same saturation range and in all tested NaCl concentrations is similar for the two samples. For both samples, a higher salinity increases the real part of the electric permittivity, the difference between drainage and imbibition electric permittivity curves, and the presence of hysteretic effect at higher frequencies. The presence of a clay fraction reduces the hysteretic effect significantly and causes the imbibition curves to lie below the drainage curves. Well-logging instruments typically work in the frequency range studied here and measure the resistivity. Utilization of the conductivity phase spectra in well logging surveys should significantly improve the sensitivity of the electric measurements to the in-situ water saturation, salinity concentration, and lithological properties of the formation. For practical purposes, the layered samples can be modeled as a series of two impedances, one is the classical parallel RC model and the second one is a distributed model that accounts for surface polarization effects. The agreement between the experimental data and model predictions is good for the range of salt concentrations used here.

Acknowledgments

We thank H.K.J. Heller and F.C. Riem Vis for technical support and Delft Earth and Shell for funding the project.

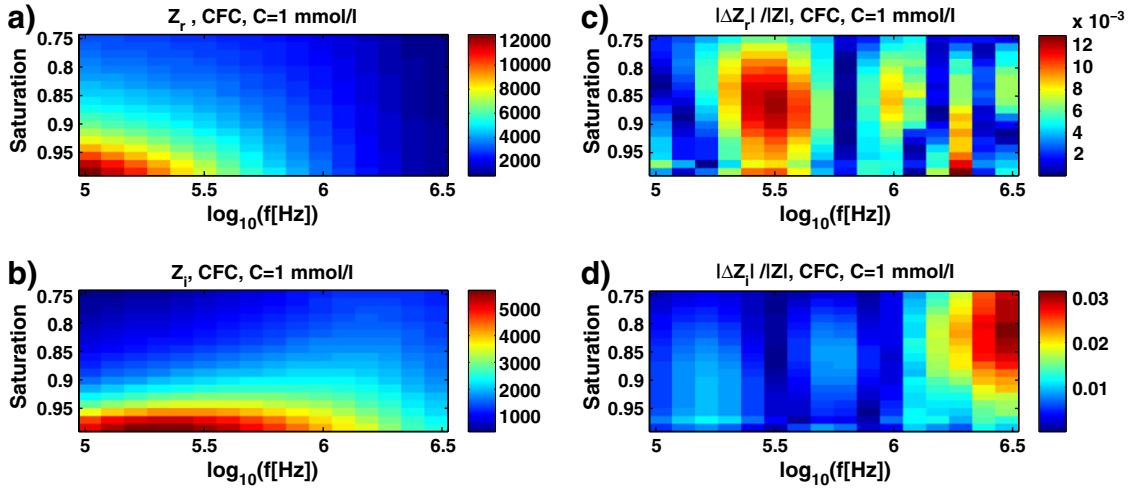

Fig. 6. Images of the real (a) and imaginary (b) parts of the electric impedance during imbibition as a function of frequency and saturation for the three-layered sand pack (CFC). The NaCl concentration was 1 mmol/l. On the right, we show the relative errors between the experimental data and our model for the real (c) and imaginary (d) part of the impedance.

References

Binley, A., Slater, L.D., Fukes, M., Cassiani, G., 2005. Relationship between spectral induced polarization and hydraulic properties of saturated and unsaturated sandstone. Water Resources Research 41, 1–13.

Chelidze, T.L., Gueguen, Y., 1999. Electrical spectroscopy of porous rocks: a review—I. Theoretical models. Geophysical Journal International 137, 1–15.

Chelidze, T.L., Gueguen, Y., Ruffet, C., 1999. Electrical spectroscopy of porous rocks: a review—II. Experimental results and interpretation. Geophysical Journal International 137, 16–34.

Garrouch, A.A., Sharma, M.M., 1994. The influence of clay content, salinity, stress, and wettability on the dielectric properties of brine-saturated rocks: 10 Hz to 10 MHz. Geophysics 59, 909–917.

Ghorbani, A., Cosenza, P.C., Revil, A., Zamora, M., Schmutz, M., Florsch, N., Jougnot, D., 2009. Non-invasive monitoring of water content and textural changes in clay-rocks using spectral induced polarization: a laboratory investigation. Applied Clay Science 43, 493–502.

Kavian, M., Slob, E.C., Mulder, W.A., 2011. Hysteresis in the nonmonotonic electric response of homogeneous and layered unconsolidated sands under continuous flow conditions with water of various salinities, 100 kHz to 2 MHz. Journal of Geophysical Research 116, B08214.

Kemna, A., Binley, A., Ramirez, A., Daily, W., 2000. Complex resistivity tomography for environmental applications. Chemical Engineering Journal 77, 11–18.

Klein, J.D., Sill, W.R., 1982. Electrical properties of artificial clay-bearing sandstone. Geophysics 47, 1593–1605.

Knight, R.J., 1991. Hysteresis in the electrical resistivity of partially saturated sandstones. Geophysics 56, 2139–2147.

Knight, R.J., Nur, A., 1987. Geometrical effects in the dielectric response of partially saturated sandstones. The Log Analyst 28, 513–519.

Kruschwitz, S., Binley, A., Lesmes, D., Elshenawy, A., 2010. Textural controls on low-frequency electrical spectra of porous media. Geophysics 75, WA113–WA123.

Lima, O.A.L., Sharma, M.M., 1992. A generalized Maxwell–Wagner theory for membrane polarization in shaly sands. Geophysics 57, 431–440.

Lou, Y., Zhang, G., 1998. Theory and application of spectral induced polarization. Geophysical Monograph Series, Society of Exploration Geophysicists 8, 1–11.

Marshall, D.J., Madden, T.R., 1959. Induced polarization, a study of its causes. Geophysics 24, 790–816.

Olhoeft, G.R., 1985. Low-frequency electrical properties. Geophysics 50, 2492–2503.

Pelton, W.H., Ward, S.H., Hallof, P.G., Sill, W.R., Nelson, P.H., 1978. Mineral discrimination and removal of inductive coupling with multi-frequency IP. Geophysics 43, 588–609.

Plug, W.J., Bruining, J., 2007. Capillary pressure for the sand–CO2–water system under various pressure conditions. Application to CO2 sequestration. Advances in Water Resources 30, 2339–2353.

Plug, W.J., Slob, E.C., Bruining, J., Tirado, L.M.M., 2007a. Simultaneous measurement of hysteresis in capillary pressure and electric permittivity for multiphase flow through porous media. Geophysics 72, A41–A45.

Plug, W.J., Slob, E.C., van Turnhout, J., Bruining, J., 2007b. Capillary pressure as a unique function of electric permittivity and water saturation. Geophysical Research Letters 34, 1–5.

Schön, J.H., 1996. Physical properties of rocks—fundamentals and principles of petrophysics. Handbook of geophysical exploration, Seismic Exploration, 18. Elsevier Science Ltd.

Shahidi, M., Hasted, J.B., Jonscher, A.K., 1975. Electrical properties of dry and humid sand. Nature 258, 595–597.

Ulrich, C., Slater, L.D., 2004. Induced polarization measurements on unsaturated, unconsolidated sands. Geophysics 69, 762–771.

Vanhala, H., Soininen, H., 1995. Laboratory techniques for measurement of spectral induced polarization response of soil samples. Geophysical Prospecting 43, 655–676.

Vinegar, H.J., Waxman, M.H., 1984. Induced polarization of shaly sands. Geophysics 49, 1267–1287.

Ward, S.H., 1990. Resistivity and induced polarization methods. In: Ward, S.H. (Ed.), Geotechnical and Environmental Geophysics: Soc. Expl. Geophys., vol. I, pp. 147–189.

Ward, S.H., Fraser, D.C., 1967. Conduction of electricity in rocks. In: Hansen, D.A., Heinrichs Jr., W.E., Holmer, R.C., MacDougall, R.E., Rogers, G.R., Sumner, J.S., Ward, S.H. (Eds.), Mining Geophysics: Soc. Expl. Geophys., vol. II, pp. 197–223.

Weller, A., Slater, L., Nordsiek, S., Ntarlagiannis, D., 2010. On the estimation of specific surface per unit pore volume from induced polarization: a robust empirical relation fits multiple data sets. Geophysics 75, WA105–WA112.